Seismic Attenuation Imaging in the Western Part of the North Anatolian Fault Zone

Wei-Mou Zhu[1,2], Luca De Siena[3], Lian-Feng Zhao[1,4], David G. Cornwell[5], Xiao-Bi Xie[6], Simona Gabrielli[7], Aqeel Abbas[8], Xi He[1], Lei Zhang[9], Panayiota Sketsiou[5], Stella Lamest[10], and Zhen-Xing Yao[1]

[1]Key Laboratory of Earth and Planetary Physics, Institute of Geology and Geophysics, Chinese Academy of Sciences, Beijing, China.
[2]College of Earth and Planetary Sciences, University of Chinese Academy of Sciences, Beijing, China.
[3]Department of Physics and Astronomy "Augusto Righi", University of Bologna, Bologna, Italy.
[4]Heilongjiang Mohe Observatory of Geophysics, Institute of Geology and Geophysics, Chinese Academy of Sciences, Beijing, China.
[5]Department Geology and Geophysics, University of Aberdeen, Aberdeen, UK.
[6]Institute of Geophysics and Planetary Physics, University of California at Santa Cruz, CA95064, USA.
[7]Istituto Nazionale di Geofisica e Vulcanologia, Sezione di Roma, Roma, Italy.
[8]Earth and Environmental Sciences Programme, The Chinese University of Hong Kong, Shatin, Hong Kong, China.
[9]School of Earth and Space Sciences, Institute of Theoretical and Applied Geophysics, Peking University, Beijing, China.
[10]Institute of Geosciences, Johannes Gutenberg University, Mainz, Germany.

Introduction

Colossal and devastating earthquakes are typically associated with the slip and rupture of fault zones. Fault zone imaging is challenging yet crucial to understand fault structure and behavior, and consequently hazard assessment and mitigation. Seismic attenuation imaging provides constraints on the fault zone structure that are independent of seismic velocity imaging. Here, we image the S-wave total attenuation structure of the western part of the North Anatolian Fault Zone (NAFZ) using data recorded by the DANA (Dense Array for North Anatolia) array (Figure 1).

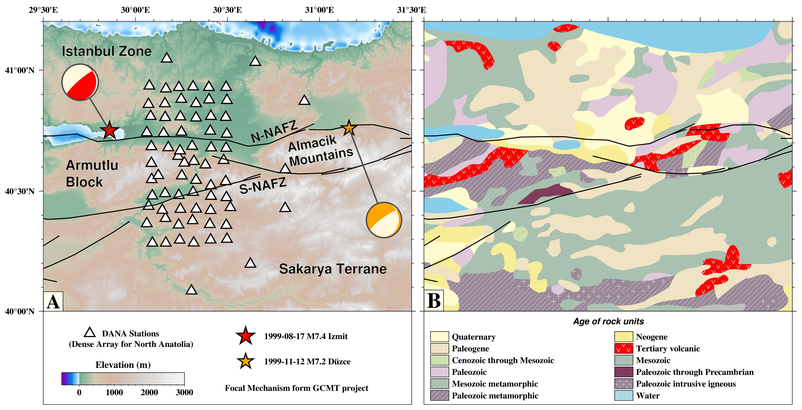

Figure 1. A: Topographic and faults map of the western part of NAFZ. Seismic stations of DANA are indicated by triangles; **B:** The simplified geological units (Pawlewicz et al., 1997)

Data and Method

Based on the event catlog form Poyraz et al., (2015), we select vertical components of the recordings for an ideal signal-to-noise ratio from the DANA array. Furthermore, the waveforms underwent a visual inspection to ensure quality control, and the arrival times for both P and S waves were picked, resulting in a final input dataset comprising a total of 3620 waveforms. MuRAT packages were used for inverted direct-wave energies based the Coda Normalization (CN) method (Sketsiou et al., 2021), and employed the seismic velocity model for ray tracing during the 3D inversion. This approach allowed us to image 3D attenuation structure of the western part of the NAFZ.

MuRAT
https://lucadesiena.github.io/MuRAT

The attenuation measurements were conducted at central frequencies of 3.0 and 6.0 Hz, based on the time-frequency analysis of all input waveforms, with an example shown in Figure 2.

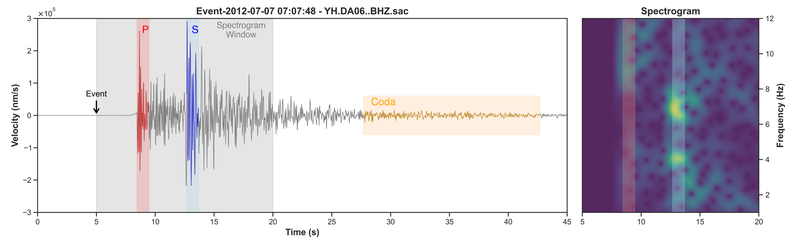

Figure 2. An example waveform illustrates the P-wave, S-wave and coda window choosing for the CN method, and the associated spectrogram.

We utilized MuRAT to invert coda-normalized direct-wave energies for total attenuation (Figure 3) and to subsequently invert attenuation values into 3D (e.g., Talone et al., 2023). This process incorporated ray-dependent sensitivity along the raypath (Figure 4), employing the seismic velocity models (Kaviani et al.,2020; Turunçtur et al., 2023).

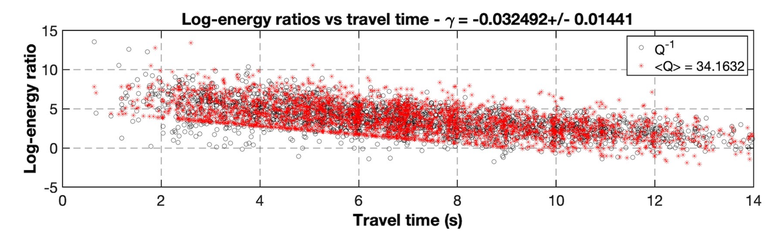

Figure 3. The log-energy ratio verses the travel time.

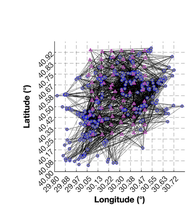

Figure 4. Raypath coverage.

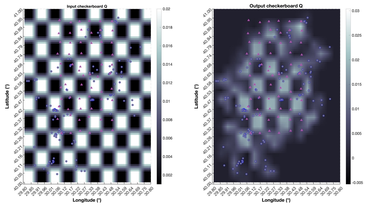

Figure 5. Checkerboard test.

Checkerboard and spike tests for this method show differences in resolution across the entire region and for interpreted anomalies (Figure 5).

3D Attenuation Structure and other observations

The attenuation variation corresponds well to the complex western NAF faults system., especially high attenuation existing in the conjunction of faults. The faults intersection between Armutlu Block and Almacik Mountain exhibits much higher attenuation compared to the other two regions. The anomaly body has a high attention value of 0.01 with a notable 3D distribution pattern: It extends from 30.2 °*E* to 30.6 °*E* and around roughly 40.6 °*N* following the northern strand of the NAF and shows a west-east trend, dipping deeper into the crust to the east from depths of 5 to 15 km (Figure 6).

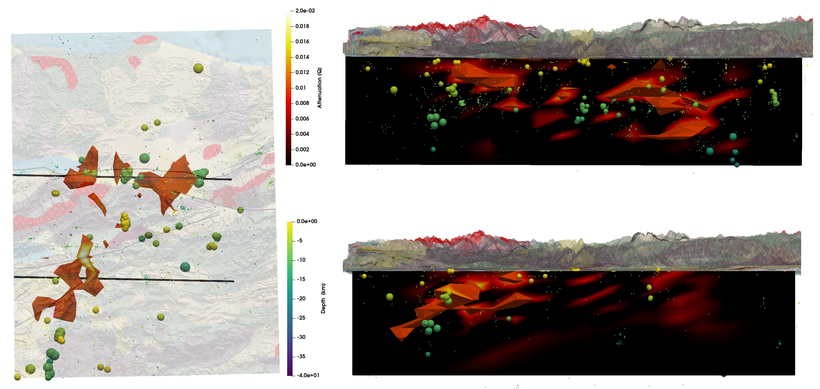

Figure 6. Maps and cross-sections of total attenuation parameter (Q). Red body is a high attenuation anomaly with a value of 0.01. The dots show the location of micro-seismicity (Beaucé et al., 2022).

This high attention anomaly corresponds well to the micro-seismicity which indicates the mechanical state of the western of NAF (Beaucé et al., 2022). Combining previous geological, geodetic and other geophysical observations, we inferred that the high values are a sign of fluid pathways. Micro-seismicity and strain distributions around the Armutlu Block are in line with the assumption fluids migrate through cracks and increased permeability attributed to the background stress.

Bibliography

Altuncu Poyraz, S., Teoman, M. U., Türkelli, N., Kahraman, M., Cambaz, D., Mutlu, A., et al. (2015). New constraints on micro-seismicity and stress state in the western part of the North Anatolian Fault Zone: Observations from a dense seismic array. *Tectonophysics*, *656*, 190–201. https://doi.org/10.1016/j.tecto.2015.06.022

Beaucé, E., van der Hilst, R. D., & Campillo, M. (2022). Microseismic Constraints on the Mechanical State of the North Anatolian Fault Zone 13 Years After the 1999 M7.4 Izmit Earthquake. *Journal of Geophysical Research: Solid Earth*, *127*(9). https://doi.org/10.1029/2022JB024416

Kaviani, A., Paul, A., Moradi, A., Mai, P. M., Pilia, S., Boschi, L., et al. (2020). Crustal and uppermost mantle shear wave velocity structure beneath the Middle East from surface wave tomography. *Geophysical Journal International*, *221*(2), 1349–1365. https://doi.org/10.1093/gji/ggaa075

Sketsiou, P., De Siena, L., Gabrielli, S., & Napolitano, F. (2021). 3-D attenuation image of fluid storage and tectonic interactions across the Pollino fault network. *Geophysical Journal International*, *226*(1), 536–547. https://doi.org/10.1093/gji/ggab109

Talone, D., De Siena, L., Lavecchia, G., & De Nardis, R. (2023). The Attenuation and Scattering Signature of Fluid Reservoirs and Tectonic Interactions in the Central-Southern Apennines (Italy). *Geophysical Research Letters*, *50*(22), e2023GL106074. https://doi.org/10.1029/2023GL106074

Weiss, J. R., Walters, R. J., Morishita, Y., Wright, T. J., Lazecky, M., Wang, H., et al. (2020). High-Resolution Surface Velocities and Strain for Anatolia From Sentinel-1 InSAR and GNSS Data. *Geophysical Research Letters*, *47*(17), e2020GL087376. https://doi.org/10.1029/2020GL087376